Title
Chemical shift assignments of mouse HOXD13 DNA binding domain bound to duplex DNA

Permalink
https://escholarship.org/uc/item/4tw5n02t

Journal
Biomolecular NMR Assignments, 9(2)

ISSN
1874-2718

Authors
Turner, Matthew
Zhang, Yonghong
Carlson, Hanqian L
et al.

Publication Date
2015-10-01

DOI
10.1007/s12104-014-9589-4

Peer reviewed

Chemical Shift Assignments of Mouse HOXD13 DNA Binding Domain Bound to Duplex DNA

Matthew Turner[1], **Yonghong Zhang**[1], **Hanqian L. Carlson**[2], **H. Scott Stadler**[2,3], and **James B. Ames**[1,*]

[1]Department of Chemistry, University of California, Davis, CA 95616

[2]Shriners Hospital for Children Research Department, 3101 SW Sam Jackson Park Road, Portland, OR 97239

[3]Department of Molecular and Medical Genetics, Oregon Health and Science University, 3181 SW Sam Jackson Park Road, Portland, OR 97239

Abstract

The homeobox gene (Hoxd13) codes for a transcription factor protein that binds to AT-rich DNA sequences and controls expression of proteins that control embryonic morphogenesis. We report NMR chemical shift assignments of mouse Hoxd13 DNA binding domain bound to an 11-residue DNA duplex (BMRB no. 25133).

Keywords

HOXD13; Homeodomain; DNA binding domain; NMR; duplex DNA

Biological Context

Homeobox (Hox) genes encode a conserved family of transcription factor proteins that are critically important in vertebrate development (Krumlauf, 1994). In humans, the Hox genes are distributed into four linkage groups (HOXA, B, C, D) comprising 39 genes located on chromosomes 7, 17, 12, and 2. At the 5′ ends of the HOXA and HOXD linkage groups are HOXA13 and HOXD13, two paralogous genes that are expressed in similar temporal and spatial domains in the developing hand, foot, and genitourinary tissues (Dolle et al., 1991, Fromental-Ramain, 1995, Knosp et al., 2004, Knosp et al., 2007, Perez et al., 2010). In humans, mutations in HOXA13 and HOXD13 cause several developmental syndromes including Hand-Foot-Genital- (HFGS) (HOXA13), Guttmacher- (GS) (HOXA13) and Synpolydactyly- (SPD) (HOXD13) which affect the formation of skeletal elements in the hand and foot as well as the formation of the external genitalia, uterus, ureter, and bladder (Poznanski et al., 1970, Innis et al., 2002; Jorgensen et al., 2010; Mortlock and Innis, 1997, Goodman, 2002, Muragaki et al., 1986).

[*]To whom correspondence should be addressed: jbames@ucdavis.edu.

A comparison of the phenotypes associated with HFGS, GS, and SPD indicate a distinct function for HOXA13 and HOXD13 in these tissues. Notably, individuals affected by SPD exhibit additional production of skeletal and soft tissues in the hand and foot resulting in extra digits that are often fused and fusions of the joints. In contrast, HFGS and GS patients often exhibit the opposite phenotype, resulting in fewer skeletal elements in the hand and foot as well as reductions in digit size (Mortlock and Innis, 1997, Goodman, 2002, Muragaki et al., 1986). Analysis of the DNA bound by HOXA13 and HOXD13 revealed important sequence differences that may explain the unique phenotypes in HFGS, GS, and SPD patients. For HOXA13, a 5′-ATAA-3′ core motif is preferred whereas HOXD13 binds to 5′-TTAT-3′, suggesting a unique mechanism for each protein to regulate the normal development of the hand, foot, and genitourinary regions. Indeed, analysis of HOXA13 and HOXD13 in the limb revealed they have distinct transcriptional targets: HOXA13 regulates Bmp2, Bmp7, Sostdc1, and Aldh1a2, to facilitate digit growth (Knosp et al., 2007, Knosp et al., 2004). By contrast, HOXD13 regulates Hand2, Fbn1, Meis1, Meis2, and Bmp4 to regulate digit number, separation, and patterning (Salsi et al., 2008).

We recently solved the NMR structure of the HOXA13 DNA binding domain (A13DBD) bound to an 11-residue DNA duplex (Zhang et al., 2011). The structure revealed hydrophobic side-chains of I53 and V60 make important sequence-specific contacts with thymine methyl groups in the DNA major groove. Residues R11 and Y14 make contacts in the minor groove. Since these residues are conserved in HOXD13 and both proteins share nearly 70% sequence identity, it is not clear how the structurally similar HOXA13 and HOXD13 can recognize such different DNA sequences. To gain insight into the sequence-specific DNA recognition by HOXD13, an atomic-resolution structure of HOXD13 bound to duplex DNA is needed to define which amino acids interact with DNA. Here we report the NMR assignments of the mouse HOXD13 DNA binding domain bound to an 11-residue DNA duplex, forming a complex called, D13DBD-DNA. The NMR assignments of D13DBD-DNA are an important first step toward elucidating the amino acids necessary for sequence specific DNA binding and provide a functional explanation for the loss of HOXD13 function in SPD.

Methods and Experiments

Preparation of HOXD13 DNA Binding Domain bound to duplex DNA (D13DBD-DNA)

A cDNA of Mus musculus HOXD13 DNA binding domain (D13DBD) was subcloned in pET-15b vector (Novagen) at Nde1 and BamH1 restriction sites that produced recombinant D13DBD with an N-terminal His(6)-tag. Thrombin cleavage of the His(6)-tag produced a polypeptide that contained 68 native residues (residues 272-339) with 6 non-native residues appended at the N-terminus (Gly-Ser-His-Met-Leu-Glu). The entire amino acid sequence of the cleaved protein is:

GSHMLEGRKKRVPYTKLQLKELENEYAINKFINKDKRRRISAATNLSERQVTIWFQ NRRVKDKKIVSKLKDTVS.

Uniformly ^{15}N-labeled and ^{13}C,^{15}N-labeled D13DBD were prepared as described previously (Zhang et al., 2009). Two complementary single strands of DNA (1: 5′-

CAACGTTAAAAC -3′ and 2: 5′-GTTTTAACGTTG -3′ purchased from _Bioneer Inc._) were synthesized and HPLC purified. For duplex DNA preparation, the two complementary DNA single strands were dissolved in 1x TE buffer (10mM TrisHCl, 1mM EDTA, pH7.5), mixed in 1:1 molar ratio, and annealed at 95°C for 10 minutes, and then cooled down to room temperature. An aliquot of duplex DNA was added to a stock solution of D13DBD in a 1:1 molar ratio and incubated at 15°C for one hour and the complex was further purified by gel-filtration size-exclusion chromatography (Superdex-75).

NMR spectroscopy

Samples of D13DBD-DNA for NMR analysis were prepared as described above, and exchanged into a buffer containing 20 mM sodium phosphate (pH 7.0) and 95% H_2O/5% D_2O, and finally concentrated to 0.3 ml giving a final protein concentration of 0.5 mM. All NMR experiments were performed at 310K on a Bruker Avance 800 MHz spectrometer equipped with a four channel interface and triple resonance cryogenic (TCI) probe. The ^{15}N-^1H HSQC spectrum (Fig. 1) was recorded with 256×2048 complex points for ^{15}N(F1) and ^1H(F2). Assignment of backbone resonances was obtained by analyzing the following spectra: HNCA, HNCACB, CBCA(CO)NH, HNCO. Side-chain assignments were obtained by analyzing constant-time ^{13}C-^1H HSQC, ^{13}C-edited NOESY-HSQC (mixing time of 120 ms) and HCCH-TOCSY experiments as described previously (Muhandiram et al., 1993). The NMR data were processed using NMRPipe and analyzed using Sparky.

Assignments and Data Deposition

Figure 1A presents the ^{15}N-^1H HSQC spectrum of ^{15}N-labeled D13DBD bound to unlabeled duplex DNA (called D13DBD-DNA) at pH 7.0 to illustrate representative backbone resonance assignments. Side-chain assignments are shown in Fig. 1B. NMR assignments were based on 3D heteronuclear NMR experiments performed on ^{13}C/^{15}N-labeled D13DBD, containing 68 native residues (residues 272-339) with 6 non-native residues appended at the N-terminus (numbered 1–74, see Fig. 2). Nearly all non-proline residues exhibited strong backbone amide resonances with uniform intensities in the HSQC spectrum, indicative of a well-defined three-dimensional protein structure. All backbone resonances (^1HN, ^{15}N, $^{13}C\alpha$, $^{13}C\beta$, and ^{13}CO) were assigned except for four residues (R38, R39, R59, and I65) that have weak and overlapping NMR intensities. More than 80% of side-chain methyl resonances were assigned as illustrated in Fig. 1B. The chemical shift index of each assigned amino acid residue was calculated as described previously (Wishart and Sykes, 1994) and revealed three α-helices (α1: T15 – I28; α2: K34 – N45; α3: V51 – K68). The protein secondary structure closely resembles the canonical secondary structure and topology seen previously in A13DBD (Zhang et al, 2011) and other homeobox proteins (Piper et al., 1999). The chemical shift assignments (^1H, ^{15}N, ^{13}C) of the D13DBD-DNA complex have been deposited in the BioMagResBank (http://www.bmrb.wisc.edu) under accession number 25133.

Figure 2 presents the chemical shift differences between D13DBD and A13DBD. The weighted average chemical shift difference was calculated for backbone amide ^1H and ^{15}N resonances of each residue. Residues A27, I28, K34, A43, T44, N57 and R58 show the largest chemical shift differences (highlighted red in Fig. 2). These changes may be the

result of direct interaction with DNA or changes in chemical environment caused by slight differences in the amino acid sequence for A13DBD vs D13DBD (eg I28 and A43 are not conserved). Residues I53, N57 and V60 are all on the same solvent exposed surface of the C-terminal helix that make direct sequence-specific contacts inside the DNA major groove observed in previous structures of A13DBD-DNA (Zhang et al., 2011) and HoxB1-DNA (Piper et al., 1999). Indeed, N57 and V60 both show large chemical shift differences, suggesting that these residues may interact differently with the bound DNA. In the A13DBD-DNA structure, N57 and V60 interact with nucleotides in the major groove (T5 and T6*) that are not conserved in the HoxD13 DNA sequence. By contrast, I53 interacts with a conserved thymine in the major groove, consistent with its very small chemical shift difference. The large chemical shift differences for A43, T44, and R58 are somewhat surprising, because these residues do not contact DNA in the A13DBD-DNA structure. Instead, R58 (helix 3) forms a salt bridge with E23 (helix 1), and A43/T44 (helix 2) both contact residues in helix 1. The large chemical shift differences for A43, T44, and R58 suggest that the three helical interfaces could be different in D13DBD vs A13DBD.

Acknowledgments

References

Innis JW, Goodman FR, Bacchelli C, Williams TM, Mortlock DP, Sateesh P, Scambler PJ, McKinnon W, Guttmacher AE. A HOXA13 allele with a missense mutation in the homeobox and a dinucleotide deletion in the promoter underlies Guttmacher syndrome. Hum Mutat. 2002; 19:573–574. [PubMed: 11968094]

Dolle P, Izpisua-Belmonte JC, Boncinelli E, Duboule D. The Hox-4.8 gene is localized at the 5′ extremity of the Hox-4 complex and is expressed in the most posterior parts of the body during development. Mech of Dev. 1991; 36:3–13.

Fromental-Ramain C, Warot X, Messadecq N, LeMeur M, Dolle P, Chambon P. Hoxa-13 and Hoxd-13 play a crucial role in the patterning of the limb autopod. Development. 1996; 122:2997–3011. [PubMed: 8898214]

Goodman FR. Limb malformations and the human HOX genes. Am J of Med Gen. 2002; 112:256–265.

Jorgensen EM, Ruman JI, Doherty L, Taylor HS. A novel mutation of HOXA13 in a family with hand-foot-genital syndrome and the role of polyalanine expansions in the spectrum of Müllerian fusion anomalies. Fertil Steril. 2010; 94:1235–1238. [PubMed: 19591980]

Knosp WM, Saneyoshi C, Shou S, Bachinger HP, Stadler HS. Elucidation, quantitative refinement, and in vivo utilization of the HOXA13 DNA binding site. J Biol Chem. 2007; 282:6843–6853. [PubMed: 17200107]

Knosp WM, Scott V, Bachinger HP, Stadler HS. HOXA13 regulates the expression of bone morphogenetic proteins 2 and 7 to control distal limb morphogenesis. Development. 2004; 131:4581–4592. [PubMed: 15342482]

Krumlauf R. Hox genes in vertebrate development. Cell. 1994; 78:191–201. [PubMed: 7913880]

Mortlock DP, Innis JW. Mutation of HOXA13 in hand-foot-genital syndrome. Nat Genet. 1997; 15:179–180. [PubMed: 9020844]

Muhandiram DR, Farrow NA, Xu G, Smallcombe SH, Kay LE. A gradient NOESY-HSQC Experiment for Recording NOESY Spectra of Proteins Dissolved in H2O. J Magn Reson B. 1993; 102:317–321.

Muragaki Y, Mundlos S, Upton J, Olsen B. Altered growth and branching patterns in synpolydactyly caused by mutations in HOXD13. Science. 1996; 272:548–551. [PubMed: 8614804]

Perez WD, Weller CR, Shou S, Stadler HS. Survival of Hoxa13 homozygous mutants reveals a novel role in digit patterning and appendicular skeletal development. Developmental dynamics. 2010; 239:446–457. [PubMed: 20034107]

Piper DE, Batchelor AH, Chang CP, Cleary ML, Wolberger C. Structure of a HoxB1–Pbx1 Heterodimer Bound to DNA: Role of the Hexapeptide and a Fourth Homeodomain Helix in Complex Formation. Cell. 1999; 96:587–597. [PubMed: 10052460]

Salsi V, Vigano MA, Cocchiarella F, Mantovani R, Zappavigna V. Hoxd13 binds in vivo and regulates the expression of genes acting in key pathways for early limb and skeletal patterning. Developmental Biology. 2008; 317:497–507. [PubMed: 18407260]

Wishart DS, Sykes BD. Chemical shifts as a tool for structure determination. Meth Enzymol. 1994; 239:363–392. [PubMed: 7830591]

Zhang Y, Thornburg CK, Stadler HS, Ames JB. (1)H, (15)N, and (13)C chemical shift assignments of mouse HOXA13 DNA binding domain. Biomol NMR Assign. 2009; 3:199–201. [PubMed: 19888690]

Zhang Y, Larsen CA, Stadler HS, Ames JB. Structural basis for sequence specific DNA binding and protein dimerization of HOXA13. PLoS One. 2011; 6:e2306.
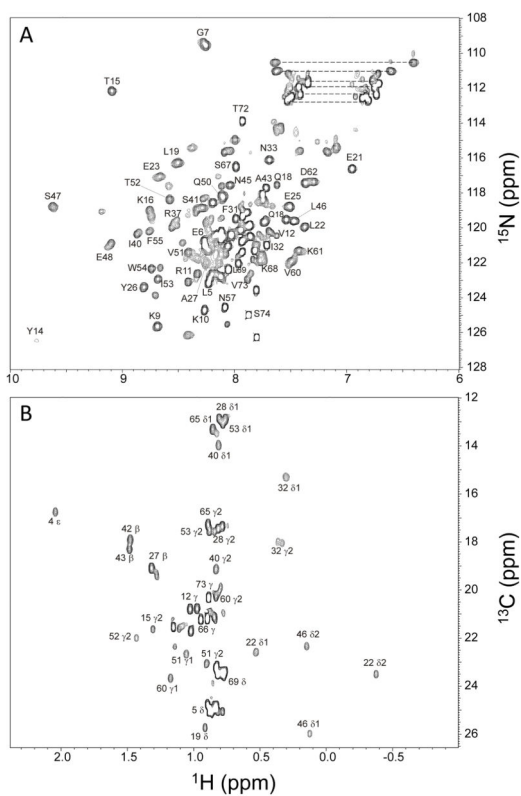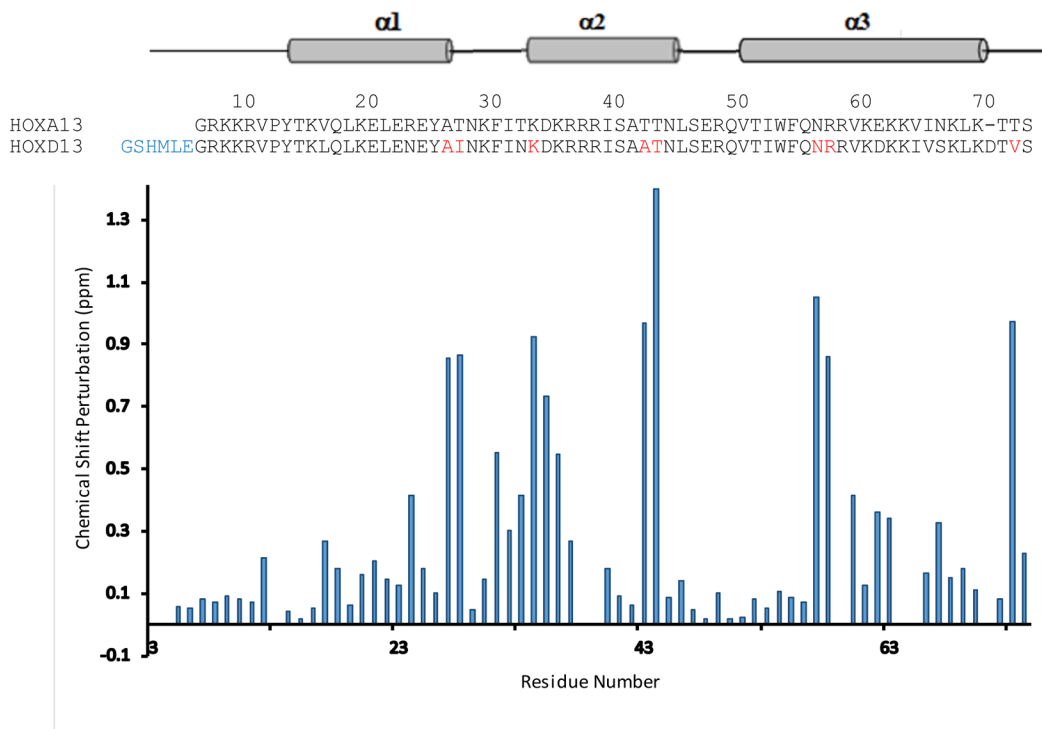
FIG. 1.
Two-dimensional ^{15}N-^1H HSQC (A) and constant-time ^{13}C-^1H HSQC (B) spectra of A13DBD-DNA at pH 7.0 recorded at 800-MHz ^1H frequency. The protein sample was uniformly labeled with ^{15}N (A) or ^{13}C (B). Amide side-chain resonances are connected by dashed lines. Resonance assignments are indicated and reported in BMRB accession no. 25133.

FIG. 2.
Secondary Structure and Chemical Shift Differences between D13DBD and A13DBB
(Wishart et al, 1994). The weighted average chemical shift differences were calculated using

$$\Delta_{av}(HN) = \sqrt{\left(\Delta H^2 + (\Delta N/5)^2\right)/2}$$ where   H and   N are chemical shift differences
between free and DNA-bound states for amide ^{1}H and ^{15}N resonances, respectively. The
secondary structure based on CSI is shown at the top (Helix 1: residues 15 - 28, Helix 2: 34 -
45, Helix 3: 51 - 68). Residues highlighted in red show the largest chemical shift difference.
Non-native residues in blue at the N-terminus remain after thrombin cleavage of the N-
terminal His(6)-tag.